*Revue des Energies Renouvelables Vol. 20 N°1 (2017) 99 - 109*
**DOI:** https://doi.org/10.54966/jreen.v20i1.613

# Direct power control of a grid connected photovoltaic system, associated with an active power filter

Mohamed Rida Bengourina [1,2], Mostefa Rahli [2] and Linda Hassaine [1]

[1] Centre de Développement des Energies Renouvelables, CDER
B.P. 62, Route de l'Observatoire, Bouzareah, 16340, Algiers, Algeria

[2] Laboratoire LORE, Faculté de Génie Electrique,
Université des Sciences et de la Technologie, Oran, Algeria

(reçu le 10 Février 2017 - accepté le 30 Mars 2017)

**Abstract** - *In this study, we present a new control method entitled direct power control without voltage sensors of a grid connected photovoltaic system associated with an active power filter. The direct control of power (DPC) is employed for the calculation of reference current generation. In this technique the switches states of inverter are selected from a table of switching based on the immediate errors between the active and reactive powers and their reference values. The objective of this paper is the reduction of Total Harmonic Distortion (THD) of source current, compensate reactive power and inject the maximum active power available from the PV array into the load and/or grid. Matlab/Simulink simulations are provided to demonstrate the performance of the proposed approach.*

**Résumé** - *Dans cette étude, nous présentons une nouvelle méthode de contrôle intitulée Contrôle direct de puissance sans capteur de tension pour un système photovoltaïque connecté au réseau associé à un filtre actif parallèle. Le contrôle direct de la puissance (DPC) est utilisé pour le calcul de la génération de courant de référence. Dans cette technique de commande, il n'y a ni boucle interne de contrôle de courant ni bloc de modulation, dans ce cas les états des interrupteurs de l'onduleur sont sélectionnés à partir d'une table de commutation basée sur les erreurs instantanées entre les puissances active et réactive estimées et leurs valeurs de références. L'objectif de cet article est la réduction de la distorsion harmonique totale (THD) du courant source, la compensation de la puissance réactive et l'injection de la puissance active maximale photovoltaïque disponible dans la charge et/ou le réseau. Des simulations Matlab/Simulink sont fournies pour démontrer la performance de l'approche propose.*

**Mots clés** - Filtre actif parallèle - DPC - Photovoltaïque - THD - Matlab - Simulink

## 1. INTRODUCTION

The growth of energy demand in the world has greatly stimulated the search for new sources of energy. Solar energy is one of the most promising non-conventional sources. Solar energy captured using photovoltaic panel represent a viable energy alternative for the production of electricity. Photovoltaic (PV) energy has great potential to supply energy with minimum impact on the environment, since it is clean and pollution free, noise-free, and renewable.

Industrial and domestic equipment use more and more electronic circuits with a nonlinear behavior. These equipments behave like nonlinear loads, generating harmonics and cause electromagnetic compatibility problems rice [1][2]. This result in the reduction of power factor, reduces the efficiency and reduces the system performs. If the grid-connected PV system is applied to non-linear loads, the power quality is relatively poorer, because of the active power supply by the PV array. To solve this problem, the grid-connected PV system should not only supply active power to the

system via MPPT, but also improve the power quality (low THD and unity power factor) [3].

In this paper, a direct coupling between the Photovoltaic cells and the shunt active power filter with direct power control (DPC) employed to inject the solar power into the utility grid under fixed Photovoltaic power conditions. The whole system can provide the power factor correction, harmonic elimination, reactive power compensation, and simultaneously inject the maximum active power available from the PV array into the load and/or grid.

The DPC strategy is based on the instantaneous active and reactive power comparators. The active power command is provided from a dc-bus voltage controller block, while the reactive power command is directly given from the outside of the controller. Errors between the commands and the estimated feedback power are input to the hysteresis comparators. Inner current control loops and PWM modulator are not required in DPC because the converter switching states are selected by a switching table based on the instantaneous errors between the commanded and estimated values of active and reactive powers [4, 5].

In order to verify the proposed system. The PV system is simulated using Simpower with S-function of Matlab/Simulink.

## 2. SYSTEM CONFIGURATION

The structure of the grid-connected PV system is shown in figure 1. The system consists of a photovoltaic array connected through a boost converter to a three-phase inverter that is connected to a grid through a simple filter and nonlinear load.

The boost converter performs the MPPT function. Whereas the inverter is used to transfer the power from PV module, it also assure the compensation of the harmonic currents, reactive power and unbalanced current.

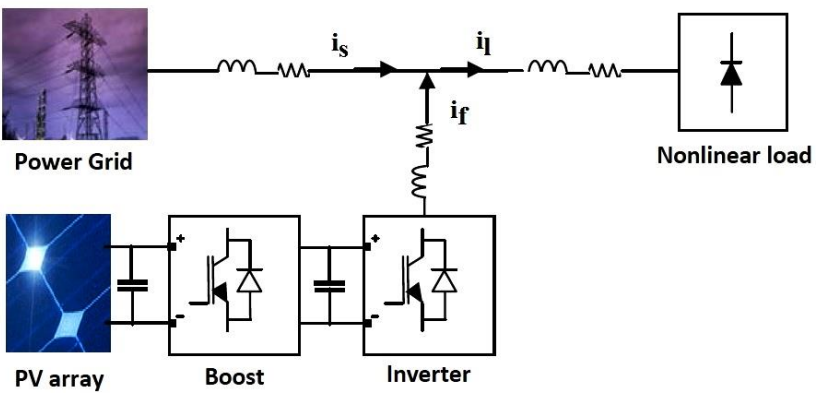


Fig. 1: Grid-connected inverter interfaced with PV system

### 2.1 PV array model

The PV module is the unity of base for the construction of a PV array. We have used the PV module model of a single diode. This model is the most commonly used due to good results [6]. The current-voltage relationship is given by:

$$I = -I_{ph} + \frac{V - R_s.I}{R_{sh}} + I_s.\left( \exp\left\{ \frac{q.(V + R_s.I)}{A\,k\,T} \right\} - 1 \right) \quad (1)$$

$I_{ph}$, the current generated by the incident light ; $I_s$, the reverse saturation or leakage current of the diode; $R_s$, the equivalent series resistance; $R_{sh}$, the equivalent parallel resistance, $q$, the electron charge ($1.60217646 \times 10^{-19}$ C); $k$, the Boltzmann constant ($1.3806503 \times 10^{-23}$ J/K); $A$, quality factor of diode.

The PV model is simulated using SunPower SPR-305E-WHT-D.

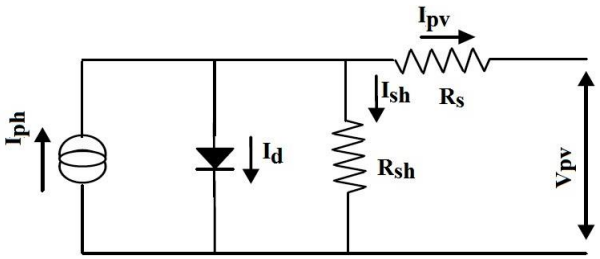


Fig. 2: Single-diode model of the theoretical PV cell

**2.2 Boost converter modeling**

Figure 3 shows the equivalent circuit of the boost converter. These converters can be described using ordinary differentiation equations as follows,

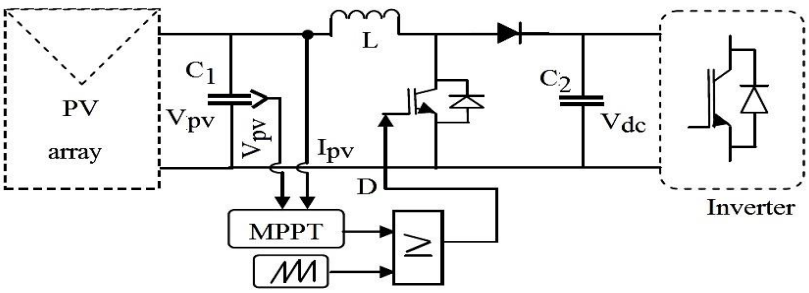


Fig. 3: Boost converter

$$I_{Lboost} = I_{pv} - C_1 . \frac{dU_{pv}}{dt} \quad (2)$$

$$I_{dc} = (1 - D) . I_{Lboost} - C_2 . \frac{dU_{dc}}{dt} \quad (3)$$

$$V_{pv} = (1 - D) . V_{dc} - L \frac{dI_{Lboost}}{dt} \quad (4)$$

$D$, is the duty cycle.

The switch is on for a period equal to $DT$, and the switch is off for an interval time equal to $(1 - D)\,T$.

**2.3 Maximum power point tracking**

Several publications on MPP methods are regularly published in the literature. For our study, we chose the MPPT algorithm of P&O. The P&O algorithm is widely used to track the maximum-power point because of its simple structure and its easy

implementation on a field-programmable gate array, [7, 8].The working principle of P&O is depicted by the flow chart in figure 4.

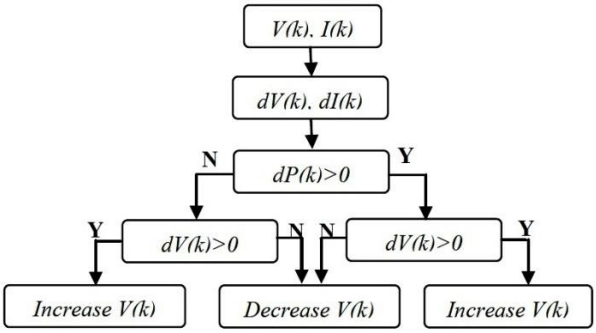


Fig. 4. P&O Algorithm

### 2.4 Active power filter

The structure of the active filter consists essentially of two parts, a power and a control part. The power part consists of an inverter, a coupling filter and a source of energy. The control part is used to control the switching of semiconductor elements forming the inverter from the power part. Au through appropriate control strategies, it is possible to generate harmonic signals at the output of the inverter to offset those present on the power grid, such as, [9]

$$i_s = i_l + i_f \tag{5}$$

$i_s$ , current of source; $i_l$ , current of the load; $i_f$ , current compensation.

## 3. DIRECT POWER CONTROL

The main idea of the direct power control (DPC) originally proposed by Ohnishi (1991) and further developed by Noguchi et al. in 1998, is similar to the direct torque control (DTC) of induction machines. Instead of flux and torque, the active power ( p ) and reactive power ( q ) are selected as two instantaneous magnitudes to control (figure 5), [10].

The estimated values of ( $p_s$ ) and ( $q_s$ ) in terms of the switching states of the converter, the three phase line currents, the dc-bus voltage, and the inductance of the reactors can be derived as, [4, 10].

$$\hat{P}_s = L\left(\frac{di_1}{dt}i_1 + \frac{di_2}{dt}i_2 + \frac{di_3}{dt}i_3\right) + V_{dc}\left(S_2 i_2 + S_2 i_2 + S_3 i_3\right) \tag{6}$$

$$\hat{q}_s = \frac{1}{\sqrt{3}};\left(3L\left(\frac{di_1}{dt}i_3 - \frac{di_3}{dt}i_1\right) - V_{dc}\left(S_1(i_2 - i_3) + S_2(i_3 - i_1) + S_3(i_1 - i_2)\right)\right) \tag{7}$$

The voltage can be estimated by the following equation

$$\begin{bmatrix} V_\alpha \\ V_\beta \end{bmatrix} = \frac{1}{i_\alpha^2 + i_\beta^2} \cdot \begin{bmatrix} i_\alpha & -i_\beta \\ i_\beta & i_\alpha \end{bmatrix} \cdot \begin{bmatrix} P_s \\ q_s \end{bmatrix} \tag{8}$$

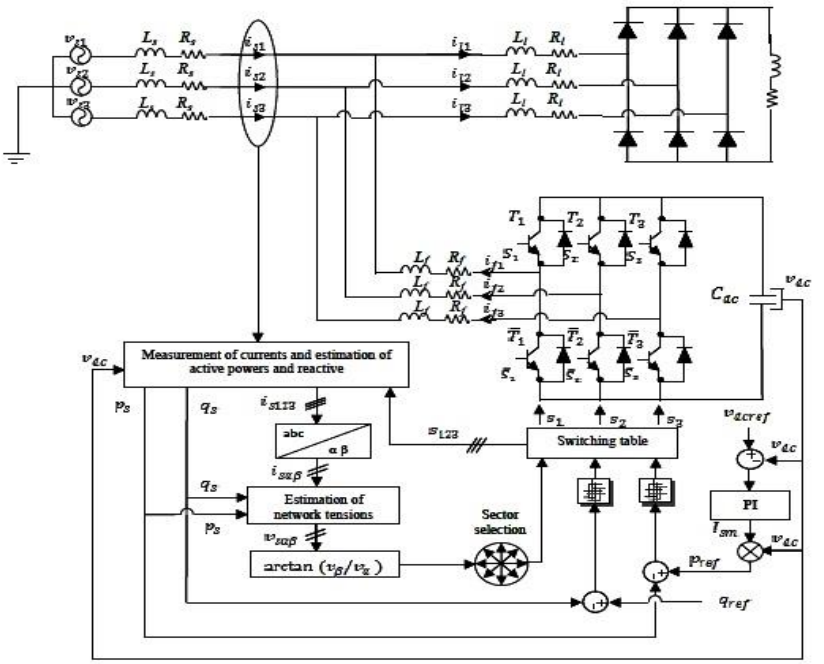


Fig. 5: General structure of shunt active filter controlled by DPC

### 3.1 Development of controllers

The reference of reactive power ( $q_{ref}$ ) and active power ( $p_{ref}$ ) are compared with the estimated reactive ( $q_s$ ) and active ( $p_s$ ). Errors between the commands and the estimated feedback power are input to the hysteresis comparators and digitized to the signals $S_p$ and $S_q$ . The output signal of the active power controller is defined.

$$\begin{cases} p_{ref} - p_s < -h_p \Rightarrow S_p = 0 \\ p_{ref} - p_s > -h_p \Rightarrow S_p = 1 \end{cases} \tag{9}$$

and similarly for the reactive power controller as,

$$\begin{cases} q_{ref} - q_s < -h_q \Rightarrow S_q = 0 \\ q_{ref} - q_s > -h_q \Rightarrow S_q = 1 \end{cases} \tag{10}$$

### 3.2 Determination of sector

The phase of the power-source voltage vector is converted to the digitized signal $\theta_N$ . For this purpose, the working plane ( $\alpha$ , $\beta$ ) is divided into 12 sectors (figure 6). The sectors can be numerically determined by the following equation, [5, 10].

$$(N-2)\frac{\pi}{6} < \theta_N < (N-1)\frac{\pi}{6} \tag{11}$$

Or, $N = 1, 2, 3,...12$ is the number of the sector.

$$\theta = \text{Arctg}\,(V_\beta)/(V_\alpha) \tag{12}$$

**Table 1**: All sectors switching table

| $S_p$ | $S_q$ | $\theta_1$ | $\theta_2$ | $\theta_3$ | $\theta_4$ | $\theta_5$ | $\theta_6$ | $\theta_7$ | $\theta_8$ | $\theta_9$ | $\theta_{10}$ | $\theta_{11}$ | $\theta_{12}$ |
|---|---|---|---|---|---|---|---|---|---|---|---|---|---|
| 1 | 0 | 101 | 111 | 100 | 000 | 110 | 111 | 010 | 000 | 011 | 111 | 001 | 000 |
| | 1 | 111 | 111 | 000 | 000 | 111 | 111 | 000 | 000 | 111 | 111 | 000 | 000 |
| 0 | 0 | 101 | 100 | 100 | 110 | 110 | 010 | 010 | 011 | 011 | 001 | 001 | 101 |
| | 1 | 100 | 110 | 110 | 010 | 010 | 011 | 011 | 011 | 101 | 101 | 101 | 100 |

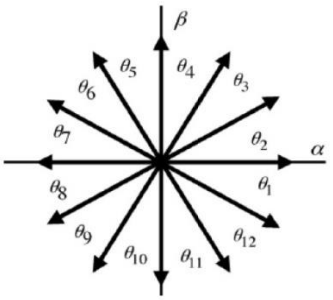


Fig. 6: Plant ( $\alpha$ , $\beta$ ) divided in 12 sector

### 3.3 Switching table

For all sectors the switching table proposed is represented in the **Table 1**.

### 3.4 PI controller

The regulation of the continuous voltage of inverter is ensured by a regulator of PI type. The error between the voltage of the capacitor $V_{dc}$ and the reference voltage $V_{dcref}$ is used as an input to PI Controller and the output is the reference active power pref. The transfer function of the PI Controller is:

$$G_{V_{dc}(PI)}(s) = \frac{k_p + s \,.\, k_i}{k.s^2 + k_p.s + k_i} \tag{13}$$

with

$$k = \frac{\sqrt{2}\,.C_{dc}\,.\,V_{dcref}}{3\,V}$$

This transfer function represents a second-order system,

So,

$$k_i = k\,.\,\omega_n^2$$

$$k_p = 2\,.\xi\,\omega_n\,.k \tag{14}$$

with, $\xi = 0.707$, $\omega_n = 2\pi f_n$

## 4. SIMULATION RESULTS AND ANALYSIS

In order to prove the performance of the Renewable Energy Interfaced Shunt Active Filter Using a flux virtual Direct Power control, the PV system depicted in figure 1 has been simulated using the SimPowerSystem with S-function of Matlab/Simulink. Parameters used in simulation are as follows.

**Table 2**. Sapf parameters

| Parameter | Value |
|---|---|
| Source voltage | 125 V |
| Supply frequency | 50 Hz |
| Source impedance $R_s$, $L_s$ | 0.1 Ω, 0.1 mH |
| Filter impedance $R_f$, $L_f$ | 0.1 Ω, 2.6 mH |
| Line impedance $R_1$, $L_1$ | 0.01 Ω, 0.5 mH |
| DC-link capacitor C | 2000 μF |
| Diode rectifier load $R_L$, $L_L$ | 20 Ω, 2 mH |

The figure 8 present the current source and there harmonic spectrum before the compensation. the current is highly distorted and its THD is equal to 27.57 %, the active and reactive power are presented in the figure 9.

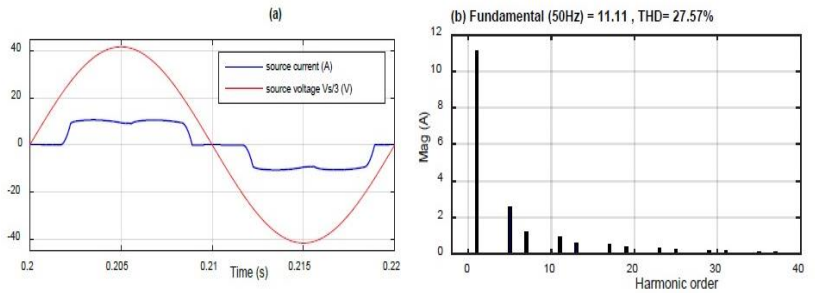


Fig. 7: (**a**) Supply current and voltage before harmonics compensation
(**b**) Current harmonic spectrum

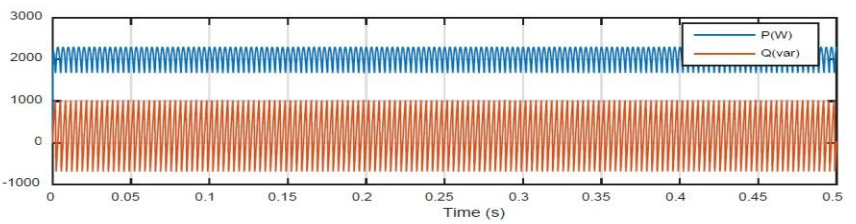


Fig. 8: Active and reactive powers of source before compensation

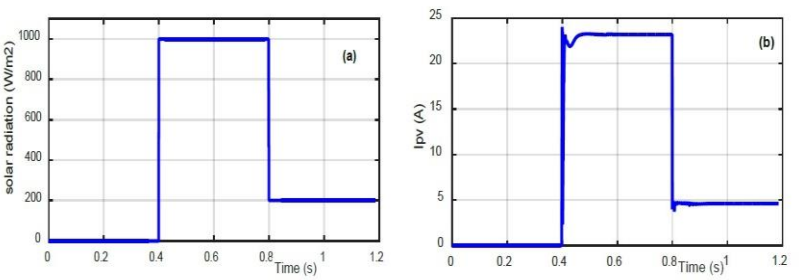


Fig. 9: (**a**) Solar radiation, (**b**) Current PV array

To verify the proposed control, a variable profile irradiance to sweep all modes of operation of our system is done. Figure 10 shows the solar irradiance level starts from 0 W/m$^2$, then increases to 1000 W/m$^2$, after that decreases to 200 W/m$^2$.

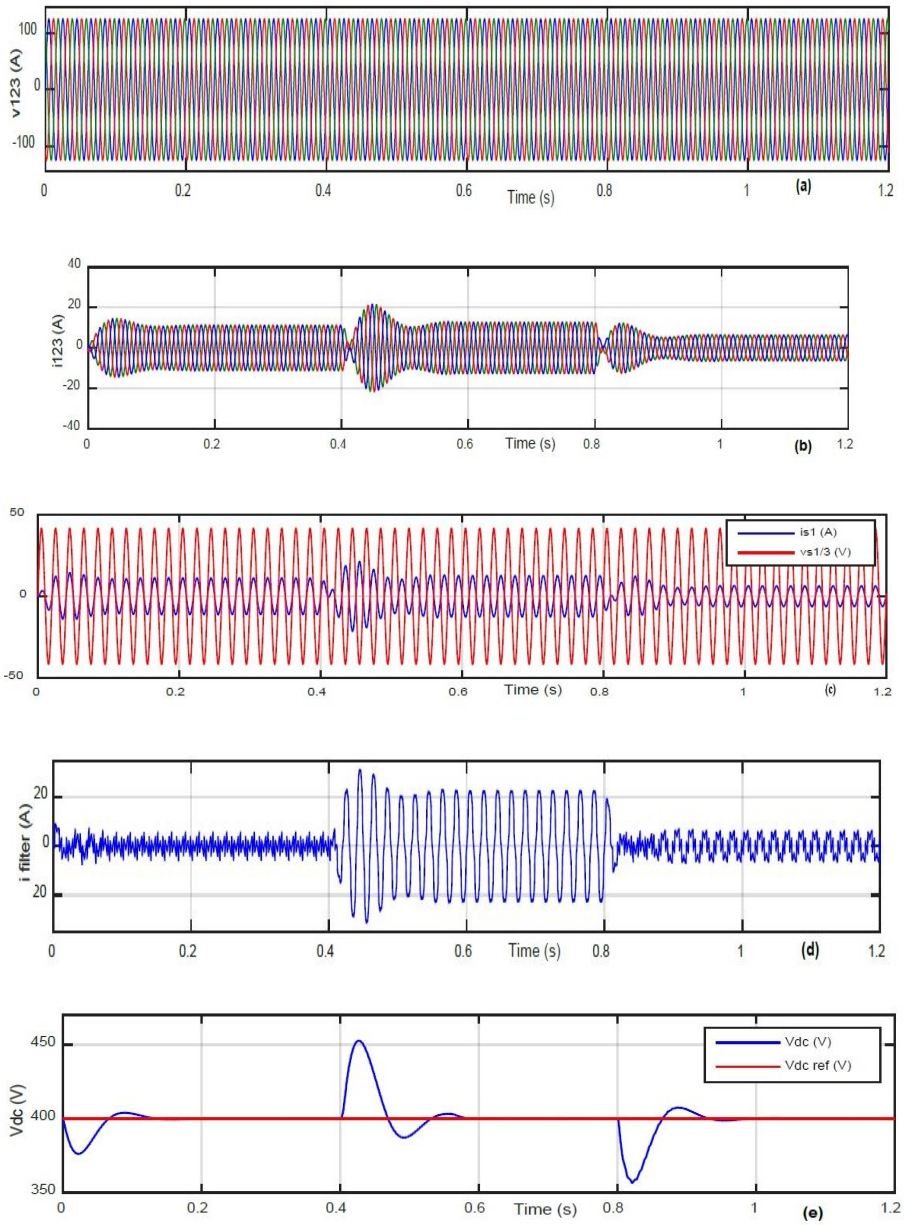


Fig. 10: Simulation results after compensation

(**a**) Source voltage, (**b**) source current, (**c**) Source voltage and current of phase 1, (**d**) Filter current, (**e**) DC-link voltage $V_{dc}$, (**f**) Active and reactive powers of source

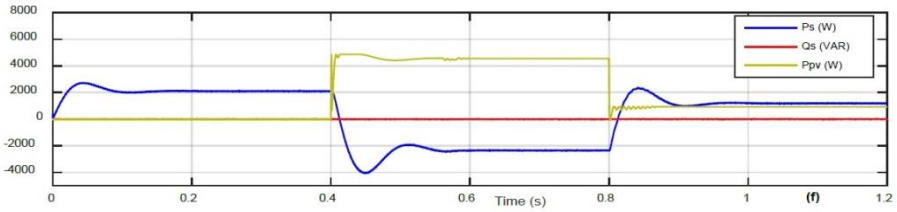


Fig. 10: Simulation results after compensation (to continue)
(**f**) Active and reactive powers of source

Figure 10 (**a**) and (**b**) show source and filter currents after filtering with PV array. The sources current become perfectly sinusoidal compensated by the filter current at unity power factor.

We can observed from 0.4 to 0.8 sec, the opposite phase between voltage and current source and the negative sign of the utility active power ( $P_S$ ), meaning the filter current has information of harmonic and PV array currents to ensure elimination of harmonic and injection of current to the load.

In figure 10 (**e**) the dc link voltage returns to its reference value in few milliseconds. The figure 10 (**f**) show the reactive and active power, the reactive power is almost kept zero, which is compensated by the reactive current injected at the PCC via the SAPF.

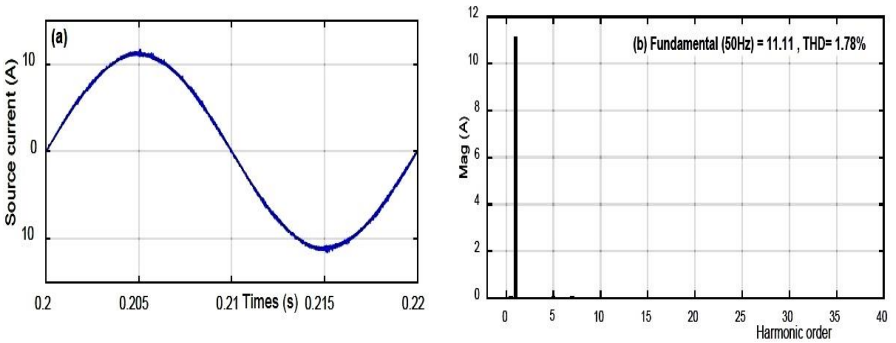


Fig. 11: (**a**) Supply current after harmonics compensation
(**b**) current harmonic spectrum

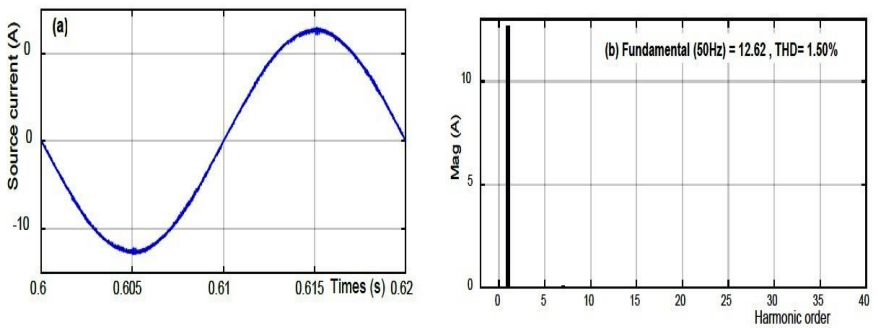


Fig. 12: (**a**) Supply current after harmonics compensation
(**b**) current harmonic spectrum

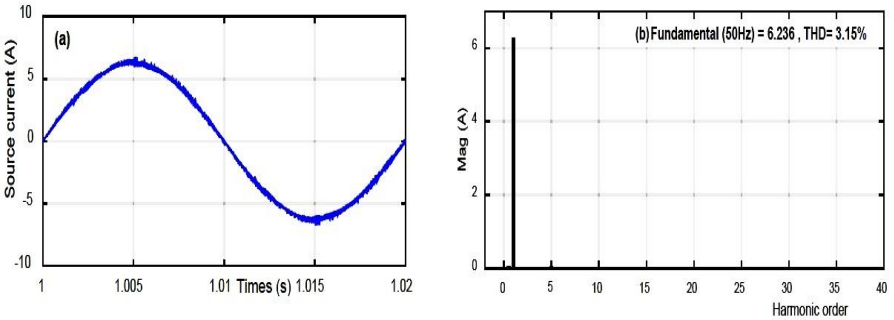


Fig. 13: (**a**) Supply current after harmonics compensation
(**b**) current harmonic spectrum

The graphs of the source current after application of the active filtering with PV array are represented on the figure 11, 12 and 13. The active filter decreases the total harmonic distortion (THD) from 27.57 % to 1.78 % with 0 W/m$^2$, 1.50 % with 1000 W/m$^2$ and 3.15 with 200 W/m$^2$; which proves the effectiveness of the proposed controller.

It can be concluded that the DPC0 gives betters results for harmonic minimization and inject the maximum active power available from the PV array into the load and/or grid.

## 5. CONCLUSION

In this paper, the validity of the proposed Direct Power Control of Active Power Filter in Grid-connected Photovoltaic Systems is investigated. The proposed system injects solar power to the grid and compensates reactive power and harmonic currents existing at PCC caused by the non-linear load. The DPC technique is employed for the calculation of reference currents containing harmonics, reactive, and solar current information. P&O algorithm is applied to optimize the power generated by the PV array and to control the DC-DC boost converter. The simulation results obtained in the various cases demonstrate the effectiveness and robustness of the proposed system.

## REFERENCES

[1] M. Haddad, S. Rahmani, A. Hamadi and K. Al-Haddad, '*New Single Phase Multilevel Reduced Count Devices to Perform Active Power Filter*', Proceedings of the IEEE SoutheastCon 2015, April, 9-12, 2015.

[2] P.N. Enjeti, W. Shireen, P. Packebush and I.J. Pitel, '*Analysis and Design of a New Active Power Filter to Cancel Neutral Current Harmonics in Three-Phase Four-Wire Electric Distribution Systems*', IEEE Transaction on Industry Application, Vol. 30, pp. 1565 – 1572, Nov /Dec 1994.

[3] S.W. Lee, J.H. Kim, S.R. Lee, B.K. Lee, and C.Y. Won, '*A Tranformerless Grid-Connected Photovoltaic System with Active and Reactive Power Control*', In Power Electronics and Motion Control Conference, IPEMC '09, pp. 2178 - 2181, 2009.

[4] M. Bouzidi, S. Bouafia, A. Bouzidi, A. Benaissa and S. Barket, '*Application of Backstepping to the Virtual Flux Direct Power Control of Five-Level Three-Phase Shunt Active Power Filter*', International Journal of Power Electronics and Drive System, IJPEDS, Vol. 4, N°2, pp. 173 - 191, 2014.

[5] A. Chaoui, J. Gaubert, and F. Karim, '*Power Quality Improvement using DPC Controlled Three-Phase Shunt Active Filter*', Electric Power Systems Research, Vol. 80, N°6, pp. 657 - 666, 2010.

[6] Marcelo Gradella Villalva, Jonas Rafael Gazoli, and Ernesto Ruppert Filho, '*Comprehensive Approach to Modeling and Simulation of Photovoltaic Arrays*', IEEE Transactions on Power Electronics, Vol. 24, N°5, pp. 1198 - 1208 .

[7] J.M. Enrique, J.M. Andujar and M.A. Bohorquez, '*A Reliable, Fast and Low Cost Maximum Power Point Tracker for Photovoltaic Applications*', Solar Energy, Vol. 84, pp. 79 – 89, 2010.

[8] E.S. Sreeraj, K. Chatterjee and S. Bandyopadhyay, '*One-Cycle-Controlled Single-Stage Single-Phase Voltage-Sensorless Grid-Connected PV System*', IEEE Transactions on Industrial Electronics, Vol. 60, N°3, pp. 1216 - 1224, 2013.

[9] K. Antoniewicz, M. Jasinski, M. Kazmierkowsk and M. Malinowski, '*Model Predictive Control for 3-Level 4-Leg Flying Capacitor Converter Operating as Shunt Active Power Filter*', IEEE Transactions on Industrial Electronics, Vol. 63, pp. 5255 – 5262, 2016.

[10] M.S. Djebbar and H. Benalla, '*Performance and High Robustness DPC for PWM Rectifier under Unstable VDC Bus*', International Journal of Power Electronics and Drive System (IJPEDS), Vol. 7, N°1, pp. 66 - 74, 2016.